HHS Public Access

Author manuscript

Int J Cancer. Author manuscript; available in PMC 2016 January 15.

Published in final edited form as:

Int J Cancer. 2015 January 15; 136(2): 476–486. doi:10.1002/ijc.29007.

Structural design of disialoganglioside GD2 and CD3-bispecific antibodies to redirect T cells for tumor therapy

Ming Cheng[1], **Mahiuddin Ahmed**[1], **Hong Xu**[1], and **Nai-Kong V. Cheung**[1,*]

[1]Department of Pediatrics, Memorial Sloan Kettering Cancer Center, 1275 York Avenue, New York, NY 10065

Abstract

Antibody based immunotherapy has proven efficacy for patients with high risk neuroblastoma. However, despite being the most efficient tumoricidal effectors, T cells are underutilized because they lack Fc receptors. Using a monovalent single chain fragment (ScFv) platform, we engineered tandem scFv bispecific antibodies (BsAbs) that specifically target disialoganglioside (GD2) on tumor cells and CD3 on T cells. Structural variants of BsAbs were constructed and ranked based on binding to GD2, and on competency in inducing T cell mediated tumor cytotoxicity. In vitro thermal stability and binding measurements were used to characterize each of the constructs, and *in silico* molecular modeling was used to show how the orientation of the variable region heavy (VH) and light (VL) chains of the anti-GD2 ScFv could alter the conformations of key residues responsible for high affinity binding. We showed that the VH-VL orientation, the $(GGGGS)_3$ linker, disulfide bond stabilization of scFv, when combined with an affinity matured mutation provided the most efficient BsAb to direct T cells to lyse GD2 positive tumor cells. *In vivo*, the optimized BsAb could efficiently inhibit melanoma and neuroblastoma xenograft growth. These findings provide preclinical validation of a structure-based method to assist in designing BsAb for T-cell mediated therapy.

Keywords

Disialoganglioside; Bispecificity; Neuroblastoma; Immunotherapy; Structure

Introduction

Neuroblastoma accounts for approximately 15% of childhood cancer mortality. Over the last two decades, tremendous progress in the understanding of neuroblastoma genetics and biology, as well as advances in therapeutic interventions, has increased the cure rate of both low- and intermediate-risk disease. However, among patients with stage 4 neuroblastoma diagnosed after 18 months of age, the prognosis is far less optimistic.[1]

[*]**Correspondence to**: Nai-Kong V. Cheung, MD PhD, Department of Pediatrics, Memorial Sloan-Kettering Cancer Center, 1275 York Avenue, New York, NY 10065. Tel No. 646-888-2313; Fax No. 631-422-0452; cheungn@mskcc.org.

Disclosure: NK Cheung is a named inventor for a patent of antibody 5F11 issued to Memorial Sloan Kettering Cancer Center. NK Cheung and M Ahmed are named inventors for a patent application of 5F11-related technology filed by Memorial Sloan Kettering Cancer Center.

T cells are effective killing machines[2] and when crosslinked to tumor cells, they are highly tumoricidal. Unfortunately, neuroblastoma has learned to escape classic T cell immunity. Yet, neuroblastoma is still vulnerable in the presence of anti-disialoganglioside (GD2) monoclonal antibody (MoAb), to nearly all classes of Fcγ receptors (FcγR) bearing effector cells, including granulocytes, natural killer cells and macrophages.[1] However, without FcγR, T cells are incapable of mediating antibody dependent cell-mediated cytotoxicity (ADCC). CD3 is an antigen on the surface of all T cells, which functions both as an activating receptor for T cells and as an anchor for bispecific antibodies (BsAb). BsAb can redirect previously-uncommitted or antigen-primed T cells to specific tumor targets,[3] forming bona fide immune synapses,[4] creating perforin pores and releasing granzymes.[5] In contrast to the canonical pathways for the generation of clonal immune cells, T cell activation by BsAb is polyclonal, MHC independent, MHC non-restricted, costimulation-independent, and with no dependency on CD4 or CD8,[4, 6] thereby overcoming the escape routes exploited by tumors during classic T cell immunotherapy.[7] BsAbs against various liquid and solid tumors have been tested in the clinic; the success of Blinatumomab, based on a monovalent tandem single chain fragment (scFv) platform, catapulted these antibody forms recently into the forefront of cancer therapy.[8-11]

GD2 is a surface glycolipid that is abundant on neuroblastoma cells,[12] and expressed at high levels in osteosarcomas, soft tissue sarcomas, retinoblastoma, small cell lung cancer, melanoma, as well as brain tumors. Its expression is restricted in normal tissues, primarily to neurons, peripheral nerves and cells in the basal layer of the skin.[13] GD2 is genetically stable and rarely lost under treatment pressure, and the majority of this antigen do not internalize after antibody binding. These features make GD2 an ideal target for MoAb based therapy. Anti-GD2 MoAbs have been successfully tested in the clinic; these include chimeric 14.18 (ch 14.18),[14] humanized 14.18 (hu 14.18),[15, 16] 3F8,[1, 17] and hu3F8.[18] Immunotherapy combining ch14.18 with GM-CSF and interleukin-2 has proven efficacy among patients with high-risk neuroblastoma.[19] Clinical trials using 3F8 with GM-CSF have also shown encouraging long term improvements in patient survival.[17]

Here we describe the generation and characterization of a series of anti-GD2 BsAbs to redirect T cells to lyse GD2 positive (GD2(+)) tumors. Our BsAbs are composed of two covalently linked scFvs, one scFv derived from anti-GD2 MoAb 5F11, another scFv derived from humanized anti-CD3 MoAb OKT3. 5F11-scFv was previously described[20] and its affinity matured by phage display.[21] The CD3-specific mouse MoAb OKT3 was the first antibody to be FDA licensed and has since been widely used clinically.[22] Here we showed that the BsAb construct (5HLDS(15)BA(Y)) with VH-VL orientation, scFv stabilization using disulfide bond, a 15-residue $(GGGGS)_3$ linker, and a high affinity mutation provided the most efficient BsAb in T-cell mediated lysis of GD2(+) tumor cells including neuroblastoma and melanoma. Cytokine release was most efficient when both BsAb and GD2(+) tumor cells were present. In vivo, 5HLDS(15)BA(Y) was highly effective in inhibiting human tumor xenograft growth.

Materials and methods

Cell lines

Neuroblastoma cell line LAN-1 and melanoma M14 were obtained from University of California, Los Angeles; NMB-7 from Dr. SK Liao of McMaster University, Hamilton, Ontario, CA. BE(1)N, and SKNJC-2 were developed at Memorial Sloan Kettering Cancer Center. The following cell lines were obtained from American Type Culture Collection (ATCC), Manassas, VA, USA: neuroblastoma, IMR-32 (CCL-127); melanoma, HT-144 (HTB63), SKMEL-1 (HTB-67), and SKMEL-28 (HTB-72); small cell lung cancer, NCI-H524 (CRL-5831), NCI-H69 (HTB-119), NCI-H196 (ATCC CRL-5823) and NCI-H345 (HTB-180); breast cancer, MDA-MB-468.

Construction of different formats of 5F11-BsAbs

The sequences of variable region of the heavy (VH) and light (VL) chains of anti-GD2 antibody 5F11,[20] and of humanized anti-CD3 OKT3 (huOKT3) were previously described.[23] 5F11-scFv genes with an orientation VH-VL or VL-VH and anti-CD3 hOKT3-scFv with an orientation VH-VL were synthesized using a 15 residue linker $((GGGGS)_3)$ (GenScript, Piscataway, NJ), and inserted into a Glutamine Synthetase (GS) mammalian expression vector to make 5F11-BsAb (5HL(15)BA and 5LH(15)BA) (BA = BsAb, **Table I**). Subsequently, two cysteine mutations, residue $S_{44}C$ on heavy chain, residue $A_{100}C$ on light chain were introduced using site-directed mutagenesis (Stratagene, CA) to stabilize[24, 25] the 5F11-scFv domains in 5HLDS(15)BA and 5LHDS(15)BA. The GS linker sequence between 5F11-scFv and hOKT3-scFv was either 15 amino acids $(GGGGS)_3$ or 5 amino acids $(GGGGS)_1$ in length, named 5HLDS(5)BA and 5LHDS(5)BA, respectively. Additionally, an affinity maturation mutation P104Y [21] was introduced into 5HLDS(15)BA to make 5HLDS(15)BA(Y).

Production and purification of 5F11-BsAbs

5F11-BsAbs DNA was transfected into DG44 CHO-S cells (Invitrogen) by electroporation using nucleofector II electroporation system (Amaxa) and nucleofection solution V. Transfected cells were subjected to drug selection with 500 μg/ml G418. Two weeks later, single cell was plated to 96-wells by serial dilution. Irradiated CHO-S cells (5000/per well) were used as feeder cells. Supernatants from clones were harvested after three weeks, and tested for GD2 binding. Clones with highest binding to GD2 were picked, and expanded in large volume culture by orbital shaking at 125 rpm in 37°C (8% CO_2). Cultures were harvested when they reached desired antibody yield or when viability dropped to <40%. 5F11-BsAb proteins secreted into the culture supernatant were purified by Ni^{2+} sepharose (GE Healthcare Bio-Sciences, Sweden) and eluted with 300 mM imidazole. Proteins were further purified to >90% monomer by size exclusion chromatography (Superdex 200GL) (GE Healthcare Bio-Sciences, Sweden).

ELISA

GD2 was first coated at 1 μg/ml per well in 90% ethanol on vinyl 96-well plates at room temperature (RT) overnight. For CD3 binding, 5000/per well of Jurkat cells (100 μl in PBS)

were used to coat 96-well plates overnight. The next day, after blocking the plates with 0.5% BSA (150 μl/well), serial dilutions of the BsAb antibodies were added to the microtiter wells and incubated at RT for 2 h. Plates were washed with PBS, a mouse-anti-His-tag antibody (AbD Serotec) (1:1000 dilutions in 0.5% BSA; 100 μl/well) was added and incubated for another hour. After washing, the wells were reacted with a goat-anti-mouse-horse radish peroxidase (HRP) antibody (1:3000 dilutions in 0.5% BSA; 100 μl/well) (Jackson ImmunoResearch) and incubated at RT for 1h. Color was developed using the o-phenylenediamine substrate (Sigma) and the ODs measured at 490 nm using ELISA reader (Dynex Technologies).

Flow cytometry

T cells expanded by CD3/CD28 beads were reacted with BsAbs (1μg per 10^6 cells) for 30 min on ice. After washing, the T cells were reacted with a mouse-anti-His-tag antibody (AbD Serotec) (0.5 μg per 10^6) on ice for 30 min. A goat anti-mouse Alexa-647 conjugated antibody was finally added to the washed T cells. After 20 min of reaction, T cells were washed and analyzed by flow cytometry on the FACS Caliber (BD Biosciences, San Jose, CA)

Molecular Modeling

All molecular modeling, energy calculations, and image rendering were done using Discovery Studio 3.5 (Accelrys, San Diego, CA). A homology model of the variable region of antibody 5F11 was built using pdb structure 1PSK as a template for both the VH and VL domains (85% sequence identity). Each CDR loop was then refined using additional homologous templates shown in parentheses: L1 (3NFS, 2W9D, 2W9E), L2 (2W9D, 2W9E, 3S62), L3 (1QOK, 3NFS, 1FOR), H1 (1UYW, 1PSK, 2OZ4), H2 (1PSK, 1KTR, 1F11), and H3 (1JPT, 1K6Q, 1FGN). The final model underwent a 0.5 ns molecular dynamics simulation to reach a low energy conformation for using in docking simulations. A docked 5F11:GD2 model was generated using CDOCKER.[26] For all docking studies involving GD2, the ceramide tail was replaced by a methyl group. We have previously shown that CDOCKER is a reliable docking algorithm for predicting the docked conformations of ganglioside oligosaccharides.[27] The top docked pose, ranked by CDOCKER Interaction energy, served as the reference docked structure for different conformations of the 5F11-scFv antibody constructs. Two 5F11-scFv constructs were modeled: 5HLDS(15)BA (VH - $(GGGGS)_3$ - VL, with disulfide stabilization (DS) between H:Cys44-L:Cys100) and $5LHDS_{15}BA$ (VH - $(GGGGS)_3$ - VL, with disulfide stabilization between H:Cys44-L:Cys100), and underwent 2 ns molecular dynamics simulation using CHARMm[28] force fields. The docked GD2 molecule from the reference 5F11:GD2 model was then superimposed onto the 5HLDS and 5LHDS Scfv models, and energy minimized using CHARMm force fields.

Thermal Stability Measurements

The thermal stabilities of 5F11-BsAbs were measured by differential scanning fluorimetry using the Protein Thermal Shift assay (Life Technologies). 5F11-BsAbs (0.2 mg/mL) were mixed with Sypro Orange dye and fluorescence was monitored using a StepOnePlus quantitative PCR machine (Applied Biosystems) with a 1% thermal gradient from 25°C to

99°C. Data was analyzed using Protein Thermal Shift Software (Applied Biosystems) to calculate the Tm using the Derivative method. A single domain 5F11-scFv construct was analyzed and used to appropriately assign the correct peaks for the 5F11-scFv and OKT3-scFv in the BsAb constructs.

Cell cytotoxicity (^{51}chromium release assay)

Melanoma (SKMEL-1, M14, HT-144, SKMEL-28), neuroblastoma cells (BE(1)N, LAN-1, NMB-7, IMR-32, SKNJC-2), and small cell lung cancer (NCI-H69, NCI-H196, NCI-H345) were cultured in RPMI1640 (Cellgro) supplemented with 10% fetal bovine serum (FBS, Life Technologies) at 37°C in a 5% CO_2 humidified incubator. Adherent cells were harvested with 1x EDTA. T cells were purified from human PBMC using Pan T cell isolation kit (Miltenyi Biotec). CD3/CD28 dynabeads (Invitrogen) were then used to stimulate and expand T cells according to manufacturer's protocol. Expanded T cells were cultured and maintained in RPMI supplemented with FBS and 30 U/ml IL-2. Cell population of T cells was analyzed on FACS Calibur with anti-CD3-percep-cy5.5, anti-CD4-FITC, anti-CD8-APC and anti-CD56-PE antibodies (BD Biosciences).

Target tumor cells were labeled with sodium ^{51}Cr chromate (Amersham, Arlington Height, IL) at 100 μCi/10^6 cells at 37°C for 1 h. After the cells were washed twice, 5000 target cells/well were mixed with 50,000 effector cells (E:T=10:1) in the presence of serial dilutions of BsAb antibodies, and incubated in 96-well polystyrene round-bottom plates (BD Biosciences) in a final volume of 250 μl/well, at 37°C for 4 h. After centrifugation at 800 g for 10 min, the released ^{51}Cr in a supernatant was counted in a γ-counter (Packed Instrument, Downers Grove, IL). Percentage of specific lysis was calculated using the formula 100% (experimental cpm - background cpm)/(5% sodium dodecyl sulfate [SDS] cpm - background cpm), where cpm represented counts per minute of ^{51}Cr released. Total release was assessed by lysis with 10% SDS (Sigma, St Louis, Mo), and background release was measured in the absence of effector cells**.**

Cytokine release assay

PBMC was isolated from healthy donor blood by lymphocyte separation medium (Mediatech Inc) centrifugation. Human T cells were purified by Pan T cell isolation kit (Miltenyi Biotec). T cells (50,000/per well) was co-cultured with neuroblastoma cell IMR-32 cell (10,000/ per well) in the presence of 5F11-BsAb in 37°C in 96 well plate. Supernatants were harvested after 24 hr of culture. Concentration of four different cytokines (IL-2, IL-10, IFN-γ and TNF-α) were assessed using a ELISA based cytokine assay kit (OptEIA™ human cytokine set, BD Biosciences) according to the manufacturer's instructions.

Xenograft mouse model

The immune deficient mouse strain BALB-Rag2-/-IL-2R-γc-KO (DKO) was kindly provided by Dr. Mamoru Ito, Central Institute for Experimental Animals, Kawasaki, Japan and maintained at Memorial Sloan-Kettering Cancer Center under sterile conditions. Animals were provided with Sulfatrim food. All procedures were performed in accordance with the protocols approved by our Institutional Animal Care and Use Committee (IACUC)

and institutional guidelines for the proper and human use of animals in research. In vivo experiments were performed in 6-10 week old mice. Peripheral blood mononuclear cells (PBMC) of healthy donors were isolated from human blood (New York blood Center). Erythrocytes were depleted by incubation for 15 minutes with erythrocyte lysis buffer (Lonza), and thrombocytes removed after differential centrifugation at 100x g for 10 minutes. All fresh PBMC samples used had similar percentages (30-50% CD3(+)) of T-cell subpopulations. In the subcutaneous tumor model, purified PBMC were mixed with M14 or IMR-32 tumor cells (at 1:1 ratio) and implanted in DKO mice subcutaneously. Treatment with BsAb was initiated on day 3 for a total of 20 days. Tumor size was measured by calipers twice a week; both tumor length and width was recorded. When tumor volumes reached 2 cm^3, mice were sacrificed. For the intravenous tumor model, M14 cells (1.5 million) were injected intravenously into DKO mice, where treatment with intravenous BsAb was initiated on day 6, given daily for two weeks. PBMCs were injected intravenously on day 6 and 13. Tumor growth was assessed by luminescence once a week starting on day 2.

Results

SDS-PAGE analysis of 5F11-BsAbs

To investigate the effect of sequence structure on 5F11-BsAb function, we engineered seven versions of 5F11-BsAbs **(Table I)** to test: (1) disulfide stabilization (DS) of 5F11-scFv; (2) VH-VL (abbreviated as HL) or VL-VH (abbreviated as LH) orientation of 5F11-scFv; (3) different GS linker length (5 $(GGGGS)_1$ versus 15 $(GGGGS)_3$) between the tandem scFv; and (4) the effect of 5F11-scFv antigen affinity. Disulfide bond was designed between heavy chain variable region residue 44 (VH44) and light chain variable region residue 100 (VL100). [24, 25, 29, 30] For instance, 5HLDS(15)BA is 5F11scFv with an orientation VH-VL and disulfide bond stabilization, linked to hOKT3 scFv (HV-VL orientation) with a 15 aa $(GGGGS)_3$ linker. The affinity purified BsAbs were analyzed by SDS-PAGE under reducing conditions**.** As shown in **Supp Figure 1**, the major protein band of all 5F11-BsAbs migrated at around the predicted molecular weight of 56 kD. The purity of 5F11-BsAbs was also assessed by HPLC, all demonstrating over 90% purity **(Supp Figure 1B)**.

Antigen binding of 5F11-BsAb

Antigen binding of 5F11-BsAbs was quantified by ELISA and normalized to that of 5HLDS(15)BA (**Table II**). Based on GD2 ELISA, 5HLDS(15)BA with disulfide bond stabilization (DS) had stronger GD2 binding than 5HL(15)BA. But when 5F11-scFv orientation was switched from VH-VL (HL) to VL-VH (LH), disulfide bond interfered with GD2 binding. Using HL-DS format, the 15-residue GS linker (5HLDS(15)BA) was superior to the 5-residue GS linker (5HLDS(5)BA) in GD2 binding. In contrast, the 5 residue GS linker with the LH orientation (5LHDS(5)BA) showed superior binding to GD2 when compared to the HL orientation (5HLDS(5)BA). When ordered by intensity of GD2-binding (**Supp Table I**), each 5F11-BsAb format was significantly better than the next in rank ($p<0.01$), except for 5HLDS(5)BA vs 5LHDS(15)BA where the p value was 0.127. The binding of these constructs to CD3(+) Jurkat cells paralleled that to GD2, although when compared to the next in rank (**Supp Table I**), the difference in CD3 binding was not

significant. Similar conclusions could be drawn when CD3 binding was assayed by flow cytometry (**Table II**). Based on these rankings of binding to GD2 and Jurkat cells, the VH-VL orientation with disulfide bond stabilization and a 15 GS linker were chosen as the final platform. Using this 5HLDS(15)BA format we next tested the importance of GD2-affinity maturation (P104Y)[21] . 5HLDS(15)BA(Y) had substantially higher binding to GD2 and CD3 than parental BsAb (5HLDS(15)BA).

Molecular Modeling

To understand the differences in relative binding of the different BsAbs to the tumor antigen GD2, molecular modeling was utilized. The best GD2 binding BsAb (excluding the P104Y affinity enhancement) was 5HLDS(15)BA and the worst was 5LHDS(15)BA. Homology models were made of the 5F11-scFv units from 5HLDS(15)BA and 5LHDS(15)BA. These two constructs differed in the relative orientation of the VH and VL domains of 5F11-scFv (**Figure 1**). Molecular dynamics simulations were run to find the low energy conformations of both formats (**Figure 1A and B**). The overlaid CDR loops are shown in **Figure 1C**. The backbone conformation of the CDR loops between the 5HLDS(15)BA and 5LHDS(15)BA varied between 2.2 and 5.8 Å RMSD (Root-Mean-Square Deviation), with the largest changes seen in the H2 and L2 loops (see **Supp Table II**).

Molecular docking was utilized to investigate the binding of 5HLDS(15)BA or 5LHDS(15)BA to the oligosaccharide head group of GD2 (see **Figure 1D**). Detailed two dimensional interaction diagrams are shown in **Figure 1E and 1F**, and the per residue interaction energies of all of the CDR residues are shown in **Supp Table III**. The total interaction energies (sum of van der Waals and electrostatic interaction) of 5HLDS(15)BA:GD2 and 5LHDS(15)BA:GD2 were −100 and −70 kcal/mol, respectively. The interaction diagrams and per residue interactions showed that the majority of the 5HLDS(15)BA:GD2 interaction was due to the importance of L: Arg90 and L: Tyr93 of the L3 loop, with interaction energies of −56 and −17 kcal/mol, respectively. Both of these contacts were greatly reduced in the 5LHDS(15)BA:GD2 (**Supp Table III**), resulting in overall loss of 30 kcal/mol of interaction energy.

Thermal Stability

Using differential scanning fluorimetry, the thermal stabilities of the seven variants were measured (**Supp Table IV**). The relative orientation of the VH and VL domains of 5F11-scFv, the presence of a disulfide stabilization in the 5F11-scFv, and the linker length between the 5F11-scFv and OKT3-scFv resulted in different thermal stabilities for both the 5F11-scFv and the OKT3-scFv in the BsAb constructs. For example, the 5HLDS(15)BA, which had high binding to both GD2 and CD3, had a 5F11-scFv Tm of 69.9±0.1 7.2°C in the melting temperatures of the 5F11-scFv and OKT3-scFv domains, respectively.

Addition of an intra-domain disulfide bond to the 5F11 scFv can either enhance or diminish the overall stability of the BsAb depending on the chain orientation. For example, adding the disulfide bond to 5F11 scFv in 5HLDS(15)BA compared to 5HL(15)BA resulted in a 10.8 and 7.5°C increase in the melting temperatures of the 5F11-scFv and OKT3-scFv domains, respectively. Conversely, adding the disulfide bond to 5F11 scFv in 5LHDS(15)BA

compared to 5LH(15)BA resulted in a 10.0 and 6.5°C decrease in the melting temperatures of the 5F11-scFv and OKT3-scFv domains, respectively. Other investigators have also found that addition of an intra-domain disulfide bond can increase or decrease the thermal stability of a scFv[29].

Comparison of thermal stability with antigen binding capability shows the general trend that the higher stability 5F11 scFv domains resulted in higher GD2 binding (excluding the case of the affinity maturation mutation) and higher stability OKT3 scFv domains resulted in higher CD3 binding. The unexpected result was that upstream perturbations to the 5F11 scFv domain and linker region could result in changes to the thermal stability and antigen binding capability of the downstream OKT3 scFv.

5F11-BsAbs exhibit potent redirected T cell killing of neuroblastoma cells

To evaluate whether 5F11-BsAb could redirect T cells to kill tumors, T cell cytotoxicity on neuroblastoma cell line LAN-1 was tested in the presence of different constructs. T cells isolated from human PBMC were expanded and stimulated with CD3/CD28 beads for two weeks to become activated T cells (ATC), and analyzed by flow cytometry to determine CD3(+), CD4(+) and CD8(+) populations. In general, more than 97% of the expanded lymphocytes were CD3 positive, with 80-90% CD8(+) and 5-10% CD4(+) (data not shown). ATC did not lyse LAN-1 cells in the absence of BsAbs. As expected, 5HLDS(15)BA(Y) the strongest GD2 binder, mediated the best T cell killing to LAN-1 cells (**Figure 2**), showing a EC50 that was 10 fold lower than that of the parental 5HLDS(15)BA (0.04 nM vs 0.5 nM, **Supp Table V**). Compared to the parental 5HLDS(15)BA, 5LHDS(5)BA showed substantially weaker cytotoxicity, killing at much higher EC50 (0.7 nM). The other constructs showed even less killing potency, with corresponding higher EC50s: 16.4 nM for 5LH(15)BA, 75 nM for 5HL(15)BA, and >185 nM for both 5HLDS(5)BA and 5LHDS(15)BA (**Figure 2**). These results suggest that killing potency strongly correlated with efficiency of antigen binding (**Supp Table V**).

5HLDS(15)BA(Y) *mediated lysis of other GD2(+) tumor lines*

We extended our studies of 5HLDS(15)BA(Y) to a larger panel of tumor cell lines. Fourteen cell lines derived from human neuroblastoma, melanoma, small cell carcinoma and breast cancer were tested. GD2 expressions of individual tumor cell lines was assessed by flow cytometry and quantified by its MFI (mean fluorescence intensity). T cells were used as effectors in cytotoxicity assays. With targets expressing high GD2 (MFI > 50), such as LAN-1, NMB-7, M14, IMR-32, and BE(1)N, EC50 was ≤ 0.2 nM. For targets expressing lower levels of GD2 (MFI < 50), such as HT-144 and NCI-H69, EC50 was generally > 0.2 nM (**Table III**). SKNJC2, SKMEL28, NCI-H196, MDA-MB-468 and NCI-H345 had low to no GD2 expression; 5HLDS(15)BA(Y) mediated low level killing of SKNJC2, SKMEL28, and MDA-MB-468, but none for NCI-H196 and NCI-H345. Susceptibility of different cell lines to killing by 5HLDS(15)BA(Y) correlated with their GD2 expression (**Supp Figure 2**), except for SKMEL1 which was exceptionally sensitive for the low level of its GD2 expression. Recognizing that fresh non-stimulated T cells were usually not as efficient as cultured/stimulated T cells[31], cytotoxicity assays against IMR-32 were repeated using them

as effectors; EC50 was similar to that using stimulated T cells (0.27 nM vs 0.2 nM), although maximum lysis was lower (36% vs 58%).

Cytokine release of T cells induced by 5HLDS(15)BA(Y)

We next measured cytokine release following BsAb activation of freshly isolated T cells purified with CD3-immunobeads. After these T cells were cultured for 24 hrs in the presence of GD2(+) neuroblastoma cell line IMR-32, their supernatants were harvested and the secreted cytokines IFN-γ, TNF-α, IL-2 and IL-10 were quantitated. Moderate amounts of IFN-γ or TNF-α were detected, but no IL-2 or IL-10 when T cells were incubated with neuroblastoma cells (NB) (**Supp Figure 3,** *CON 2*). While CD3/CD28 immunobeads induced all four cytokine release to different extents (*CON 3*), the addition of neuroblastoma cells, without BsAb, further increased the release of IFN-γ and TNF-α (*CON 4*). 5HLDS(15)BA(Y) did not induce cytokine release in the absence of neuroblastoma cells. When neuroblastoma cells were present, IFN-γ and TNF-α release was substantial, while IL-10 and IL-2 were only minimally increased, if at all. Since IFN-γ and TNF-α were Th1 associated, while IL-10 were Th2-associated cytokine, 5HLDS(15)BA(Y) appeared to be selective in activating Th1 rather than Th2 cytokine, and only when both T cells and GD2(+) tumors were present.

Efficacy of 5HLDS(15)BA(Y) against human tumor xenografts

We tested the anti-tumor effect of 5HLDS(15)BA(Y) using a xenograft model where fresh human PBMCs (not cultured T cells) were used as effectors in immune deficient DKO mice.[10] Three days after PBMC mixed with tumor cells (E: T = 1:1) were implanted sc in DKO mice, treatment with 5HLDS(15)BA(Y) was initiated. This sc tumor model was chosen to simulate the recruitment of T cells in the tumor stroma[11, 32]. For *BRAF* mutated melanoma M14 (**Figure 3A**), tumor growth was evident on day 5 with no treatment, although tumor growth was delayed when PBMC was present. When 5HLDS(15)BA(Y) was added, tumor growth was effectively suppressed, with only one out of five showing growth on day 30. In a second xenograft model, PBMCs were mixed with *MYCN* amplified neuroblastoma IMR-32 and implanted sc. As shown in **Figure 3B**, tumor growth was evident by day 5; treatment with 5HLDS(15)BA(Y) achieved significant delay in tumor growth until after day 20. In a subset of animals, no observable tumor growth was observed past the end of the study on day 150. In a third tumor model, melanoma tumor cells were injected intravenously to simulate a metastatic tumor model, where 5HLDS(15)BA(Y) and PBMC were both administered intravenously on day 6 after tumor implantation. Treatment with 5HLDS(15)BA(Y) and PBMC showed near complete tumor eradication on day 17 **(Figure 3C, D)**.

Discussion

We tested the importance of structural design on the potency of anti-GD2 BsAb. We used the previously optimized anti-GD2 5F11 and the well characterized anti-CD3 OKT3 antibody systems to build BsAbs. Thermal stability correlated with antigen binding, which in turn was a powerful predictor of EC50 in directing T cell killing of GD2(+) tumor cells. Validation of the final optimized construct 5HLDS(15)BA(Y) was successful *in vitro*

against a representative panel of GD2(+) cell lines, and in vivo in three xenograft therapy models. This therapeutic candidate appears to have clinical potential as a T cell engaging BsAb, and the algorithm developed for optimizing 5F11-BsAb should be applicable for other BsAb systems.

To design 5F11-BsAb we undertook a systemic evaluation of the key variables in optimizing BsAb: 1) additional disulfide bond to stabilize the scFv[30]. 2) VH-VL or VL-VH orientation of the 5F11-scFv, and 3) linker length (5 GS versus 15 GS) between 5F11-scFv and hOKT3-scFv. With a VH-VL orientation, 15 GS linker, and disulfide stabilization of 5F11-scFv, thermal stability of the 5F11-scFv domain and the binding of 5HLDS(15)BA to GD2 were superior to that of other BsAb constructs. Molecular modeling revealed that the majority of the binding interaction between the 5HLDS(15)BA and the tumor antigen GD2 was mediated by two residues in the CDR L3 loop: Arg90 and Tyr93. L:Arg90 helped to neutralize the (−2) formal charge of the GD2 oligosaccharide head group. The docking and molecular dynamics study showed that the strong interactions of L:Arg90 and L:Tyr93 were lost in the weakest construct, 5LHDS(15)BA. This in silico prediction was confirmed experimentally by the 100-fold loss of GD2 binding for 5LHDS(15)BA relative to 5HLDS(15)BA.

With the VH-VL orientation and disulfide bond stabilization, the 15 GS linker (5HLDS(15)BA) showed superior antigen binding compared to the 5 amino acid linker (5HLDS(5)BA), suggesting the importance of flexibility between two scFvs for optimal antigen binding. As expected, addition of affinity maturation mutation P104Y (5HLDS(15)BA(Y)) further increased the antigen binding of 5HLDS(15)BA. Even though hOKT3-scFv had identical VH-VL orientations in all these 5F11-BsAb constructs, their CD3 binding varied, probably as a result of the thermal stability and the steric effect of the 5F11-scFv domain in the different formats.

These 5F11-BsAb induced T cell cytotoxicity which correlated strongly with their antigen binding capability. 5HLDS(15)BA(Y) had the best antigen binding, and it mediated T cell killing with the lowest EC50 of 40 pM. In contrast, 5HLDS(5)BA and 5LHDS(15)BA had the worst antigen binding, and they were the least efficient in tumor killing, i.e. higher EC50. Applying 5HLDS(15)BA(Y) to a series of GD2(+) neuroblastoma and melanoma cell lines, we showed that cytotoxicity was a function of GD2 expression. Tumor cell line expressing higher levels of GD2 such as NMB-7, LAN-1 and M14, were more efficiently lysed by T cells in the presence of low concentrations (low EC50) of 5HLDS(15)BA(Y). Collectively, these experiments suggest that target GD2 binding is the key determinant of BsAb potency, and could be a useful measure for high throughput screen during the process of building BsAb.

T cells activated by 5HLDS(15)BA(Y) could induce cytokine release, but most efficiently in the presence of antigen-positive tumor cells. The pattern of cytokine release, i.e. IFN-γ and TNF-α instead of IL-2 or IL10, were consistent with a Th1 profile, which should be conducive to a proinflammatory response and positive host anti-tumor immunity. The magnitude of IL-2 release was surprisingly low when T cells were activated with 5HLDS(15)BA(Y). Similar findings have been reported in the clinical trial of

blinatumomab.[33] It is reassuring since high levels of IL-2 are often involved in cytokine release syndromes in patients whose T cells are activated. However, whether cytokine storm will occur will have to await clinical testing in human patients.

5HLDS(15)BA(Y) significantly inhibited xenograft tumor growth in vivo. Although no clinical toxicity was observed, a formal toxicity study will be critical to access side effects other than cytokine storm. In xenograft studies, we chose to start 5HLDS(15)BA(Y) treatment on day 3 to day 6, instead of the same day of tumor implantation in order to be certain that tumors were engrafted and growing before the treatment was initiated. In our studies, we did not optimize the dose or the schedule, using 20 ug 5HLDS(15)BA(Y) bolus injection per day for a total of 14 to 20 days. Since these tandem scFv BsAbs generally have short serum half-lives[33], continuous infusion could yield better serum levels and probably better anti-tumor effects.

Recently, hybrid-hybridoma (quadroma) platform was used to produce a trifunctional hybrid antibody with monovalent binding to targets (GD2 and CD3), carrying a specially engineered chimeric mouse IgG2a × rat IgG2b Fc with preferential binding to activating FcγR[34, 35]. Its EC50 in vitro was 70 ng/ml (0.47 nM), substantially less optimal than that of 5HLDS(15)BA(Y). Part of the reason was most likely the low affinity of the ant-GD2 scFv ME361. Despite binding to GD2 by ELISA, ME361-scFv had insufficient signal by Biacore (data not shown), in contrast to 5F11-scFv which showed a binding KD = 1.27×10^{-7} M. Unlike the trifunctional antibody studies, our tumor model was not designed to study vaccination effect, but rather to focus solely on redirecting human T cells for tumor therapy. Whether these 5F11-BsAb can induce protective immunity will require further studies in immunocompetent systems.

Supplementary Material

Refer to Web version on PubMed Central for supplementary material.

Acknowledgement

We want to thank Dr. Mamoru Ito of Central Institute for Experimental Animals, Kawasaki, Japan, for kindly providing the DKO mice for our studies. We are grateful to Dr. Gloria Koo, Hospital for Special Surgery, New York, NY, for her expertise and advice in handling these DKO mice. We also want to thank Ms. Hongfen Guo and Dr. Jian Hu for their expert technical assistance on gel filtration.

References

1. Cheung NK, Dyer MA. Neuroblastoma: Developmental Biology, Cancer Genomics, and Immunotherapy. Nature Reviews Cancer. 2013; 13:397–411. [PubMed: 23702928]
2. Wisloff F, Froland SS, Michaelsen TE. Antibody-dependent cytotoxicity mediated by human Fc-receptor-bearing cells lacking markers for B- and T-lymphocytes. Int Arch Allergy Appl Immunol. 1974; 47:139–54. [PubMed: 4603056]
3. Wolf E, Hofmeister R, Kufer P, Schlereth B, Baeuerle PA. BiTEs: bispecific antibody constructs with unique anti-tumor activity. Drug Discov Today. 2005; 10:1237–44. [PubMed: 16213416]
4. Offner S, Hofmeister R, Romaniuk A, Kufer P, Baeuerle PA. Induction of regular cytolytic T cell synapses by bispecific single-chain antibody constructs on MHC class I-negative tumor cells. Mol Immunol. 2006; 43:763–71. [PubMed: 16360021]

5. Thiery J, Keefe D, Boulant S, Boucrot E, Walch M, Martinvalet D, Goping IS, Bleackley RC, Kirchhausen T, Lieberman J. Perforin pores in the endosomal membrane trigger the release of endocytosed granzyme B into the cytosol of target cells. Nat Immunol. 2011; 12:770–7. [PubMed: 21685908]

6. Dreier T, Baeuerle PA, Fichtner I, Grun M, Schlereth B, Lorenczewski G, Kufer P, Lutterbuse R, Riethmuller G, Gjorstrup P, Bargou RC. T cell costimulus-independent and very efficacious inhibition of tumor growth in mice bearing subcutaneous or leukemic human B cell lymphoma xenografts by a CD19-/CD3-bispecific single-chain antibody construct. J Immunol. 2003; 170:4397–402. [PubMed: 12682277]

7. Choi BD, Kuan CT, Cai M, Archer GE, Mitchell DA, Gedeon PC, Sanchez-Perez L, Pastan I, Bigner DD, Sampson JH. Systemic administration of a bispecific antibody targeting EGFRvIII successfully treats intracerebral glioma. Proc Natl Acad Sci U S A. 2013; 110:270–5. [PubMed: 23248284]

8. Bargou R, Leo E, Zugmaier G, Klinger M, Goebeler M, Knop S, Noppeney R, Viardot A, Hess G, Schuler M, Einsele H, Brandl C, et al. Tumor regression in cancer patients by very low doses of a T cell-engaging antibody. Science. 2008; 321:974–7. [PubMed: 18703743]

9. Topp MS, Kufer P, Gokbuget N, Goebeler M, Klinger M, Neumann S, Horst HA, Raff T, Viardot A, Schmid M, Stelljes M, Schaich M, et al. Targeted therapy with the T-cell-engaging antibody blinatumomab of chemotherapy-refractory minimal residual disease in B-lineage acute lymphoblastic leukemia patients results in high response rate and prolonged leukemia-free survival. J Clin Oncol. 2011; 29:2493–8. [PubMed: 21576633]

10. Schlereth B, Fichtner I, Lorenczewski G, Kleindienst P, Brischwein K, da Silva A, Kufer P, Lutterbuese R, Junghahn I, Kasimir-Bauer S, Wimberger P, Kimmig R, et al. Eradication of tumors from a human colon cancer cell line and from ovarian cancer metastases in immunodeficient mice by a single-chain Ep-CAM-/CD3-bispecific antibody construct. Cancer Res. 2005; 65:2882–9. [PubMed: 15805290]

11. Lutterbuese R, Raum T, Kischel R, Hoffmann P, Mangold S, Rattel B, Friedrich M, Thomas O, Lorenczewski G, Rau D, Schaller E, Herrmann I, et al. T cell-engaging BiTE antibodies specific for EGFR potently eliminate KRAS- and BRAF-mutated colorectal cancer cells. Proc Natl Acad Sci U S A. 2010; 107:12605–10. [PubMed: 20616015]

12. Wu ZL, Schwartz E, Seeger R, Ladisch S. Expression of GD2 ganglioside by untreated primary human neuroblastomas. Cancer Res. 1986; 46:440–3. [PubMed: 3940209]

13. Hersey P, Jamal O, Henderson C, Zardawi I, D'Alessandro G. Expression of the gangliosides GM3, GD3 and GD2 in tissue sections of normal skin, naevi, primary and metastatic melanoma. Int J Cancer. 1988; 41:336–43. [PubMed: 3346097]

14. Yu AL, Gilman AL, Ozkaynak MF, London WB, Kreissman SG, Chen HX, Smith M, Anderson B, Villablanca JG, Matthay KK, Shimada H, Grupp SA, et al. Anti-GD2 antibody with GM-CSF, interleukin-2, and isotretinoin for neuroblastoma. N Engl J Med. 2010; 363:1324–34. [PubMed: 20879881]

15. Albertini MR, Hank JA, Gadbaw B, Kostlevy J, Haldeman J, Schalch H, Gan J, Kim K, Eickhoff J, Gillies SD, Sondel PM. Phase II trial of hu14.18-IL2 for patients with metastatic melanoma. Cancer Immunol Immunother. 2012

16. Delgado DC, Hank JA, Kolesar J, Lorentzen D, Gan J, Seo S, Kim K, Shusterman S, Gillies SD, Reisfeld RA, Yang R, Gadbaw B, et al. Genotypes of NK cell KIR receptors, their ligands, and Fcgamma receptors in the response of neuroblastoma patients to Hu14.18-IL2 immunotherapy. Cancer Res. 2010; 70:9554–61. [PubMed: 20935224]

17. Cheung NK, Cheung IY, Kushner BH, Ostrovnaya I, Chamberlain E, Kramer K, Modak S. Murine Anti-GD2 Monoclonal Antibody 3F8 Combined With Granulocyte-Macrophage Colony-Stimulating Factor and 13-Cis-Retinoic Acid in High-Risk Patients With Stage 4 Neuroblastoma in First Remission. J Clin Oncol. 2012; 30:3264–70. [PubMed: 22869886]

18. Cheung NK, Guo H, Hu J, Tassev DV, Cheung IY. Humanizing murine IgG3 anti-GD2 antibody m3F8 substantially improves antibody-dependent cell-mediated cytotoxicity while retaining targeting in vivo. OncoImmunology. 2012; 1:477–86. [PubMed: 22754766]

19. Yu AL, Gilman AL, Ozkaynak MF, London WB, Kreissman SG, Chen HX, Smith M, Anderson B, Villablanca JG, Matthay KK, Shimada H, Grupp SA, et al. Anti-GD2 antibody with GM-CSF,

interleukin-2, and isotretinoin for neuroblastoma. N Engl J Med. 2010; 363:1324–34. [PubMed: 20879881]

20. Cheung NK, Modak S, Lin Y, Guo H, Zanzonico P, Chung J, Zuo Y, Sanderson J, Wilbert S, Theodore LJ, Axworthy DB, Larson SM. Single-chain Fv-streptavidin substantially improved therapeutic index in multistep targeting directed at disialoganglioside GD2. J Nucl Med. 2004; 45:867–77. [PubMed: 15136638]
21. Hu J, Huang X, Ling CC, Bundle DR, Cheung NK. Reducing epitope spread during affinity maturation of an anti-ganglioside GD2 antibody. J Immunol. 2009; 183:5748–55. [PubMed: 19812201]
22. Chatenoud L. Anti-CD3 antibodies: towards clinical antigen-specific immunomodulation. Curr Opin Pharmacol. 2004; 4:403–7. [PubMed: 15251136]
23. Adair JR, Athwal DS, Bodmer MW, Bright SM, Collins AM, Pulito VL, Rao PE, Reedman R, Rothermel AL, Xu D, et al. Humanization of the murine anti-human CD3 monoclonal antibody OKT3. Human antibodies and hybridomas. 1994; 5:41–7. [PubMed: 7858182]
24. Jung SH, Pastan I, Lee B. Design of interchain disulfide bonds in the framework region of the Fv fragment of the monoclonal antibody B3. Proteins. 1994; 19:35–47. [PubMed: 8066084]
25. Reiter Y, Brinkmann U, Lee B, Pastan I. Engineering antibody Fv fragments for cancer detection and therapy: Disulfide-stabilized Fv fragments. Nat Biotechnol. 1996; 14:1239–45. [PubMed: 9631086]
26. Wu G, Robertson DH, Brooks CL 3rd, Vieth M. Detailed analysis of grid-based molecular docking: A case study of CDOCKER-A CHARMm-based MD docking algorithm. J Comput Chem. 2003; 24:1549–62. [PubMed: 12925999]
27. Ahmed M, Goldgur Y, Hu J, Guo HF, Cheung NK. In silico Driven Redesign of a Clinically Relevant Antibody for the Treatment of GD2 Positive Tumors. PloS one. 2013; 8:e63359. [PubMed: 23696816]
28. Momany FA, Rone R. Validation of the General Purpose QUANTA 3.2/CHARMm Force Field. J Comp Chem. 1992; 13:888–900.
29. Weatherill EE, Cain KL, Heywood SP, Compson JE, Heads JT, Adams R, Humphreys DP. Towards a universal disulphide stabilised single chain Fv format: importance of interchain disulphide bond location and vL-vH orientation. Protein Eng Des Sel. 2012; 25:321–9. [PubMed: 22586154]
30. Michaelson JS, Demarest SJ, Miller B, Amatucci A, Snyder WB, Wu X, Huang F, Phan S, Gao S, Doern A, Farrington GK, Lugovskoy A, et al. Anti-tumor activity of stability-engineered IgG-like bispecific antibodies targeting TRAIL-R2 and LTbetaR. MAbs. 2009; 1:128–41. [PubMed: 20061822]
31. Molhoj M, Crommer S, Brischwein K, Rau D, Sriskandarajah M, Hoffmann P, Kufer P, Hofmeister R, Baeuerle PA. CD19-/CD3-bispecific antibody of the BiTE class is far superior to tandem diabody with respect to redirected tumor cell lysis. Mol Immunol. 2007; 44:1935–43. [PubMed: 17083975]
32. Brischwein K, Schlereth B, Guller B, Steiger C, Wolf A, Lutterbuese R, Offner S, Locher M, Urbig T, Raum T, Kleindienst P, Wimberger P, et al. MT110: a novel bispecific single-chain antibody construct with high efficacy in eradicating established tumors. Mol Immunol. 2006; 43:1129–43. [PubMed: 16139892]
33. Klinger M, Brandl C, Zugmaier G, Hijazi Y, Bargou RC, Topp MS, Gokbuget N, Neumann S, Goebeler M, Viardot A, Stelljes M, Bruggemann M, et al. Immunopharmacologic response of patients with B-lineage acute lymphoblastic leukemia to continuous infusion of T cell-engaging CD19/CD3-bispecific BiTE antibody blinatumomab. Blood. 2012; 119:6226–33. [PubMed: 22592608]
34. Ruf P, Schafer B, Eissler N, Mocikat R, Hess J, Ploscher M, Wosch S, Suckstorff I, Zehetmeier C, Lindhofer H. Ganglioside GD2-specific trifunctional surrogate antibody Surek demonstrates therapeutic activity in a mouse melanoma model. J Transl Med. 2012; 10:219. [PubMed: 23134699]

35. Eissler N, Ruf P, Mysliwietz J, Lindhofer H, Mocikat R. Trifunctional bispecific antibodies induce tumor-specific T cells and elicit a vaccination effect. Cancer Res. 2012; 72:3958–66. [PubMed: 22745368]

What's new?

The success of anti-disialoganglioside (GD2) antibody immunotherapy can be substantially enhanced if T cells are engaged by bispecific antibodies (BsAbs). We showed that structural optimization based on in silico modeling could enhance tumor cytotoxicity that correlated with GD2-binding in vitro, and efficient ablation of xenografts in the presence of human T cells. This strategy is critical for scFv-based low affinity BsAb against carbohydrates such as GD2, before their optimal therapeutic potential can be realized.

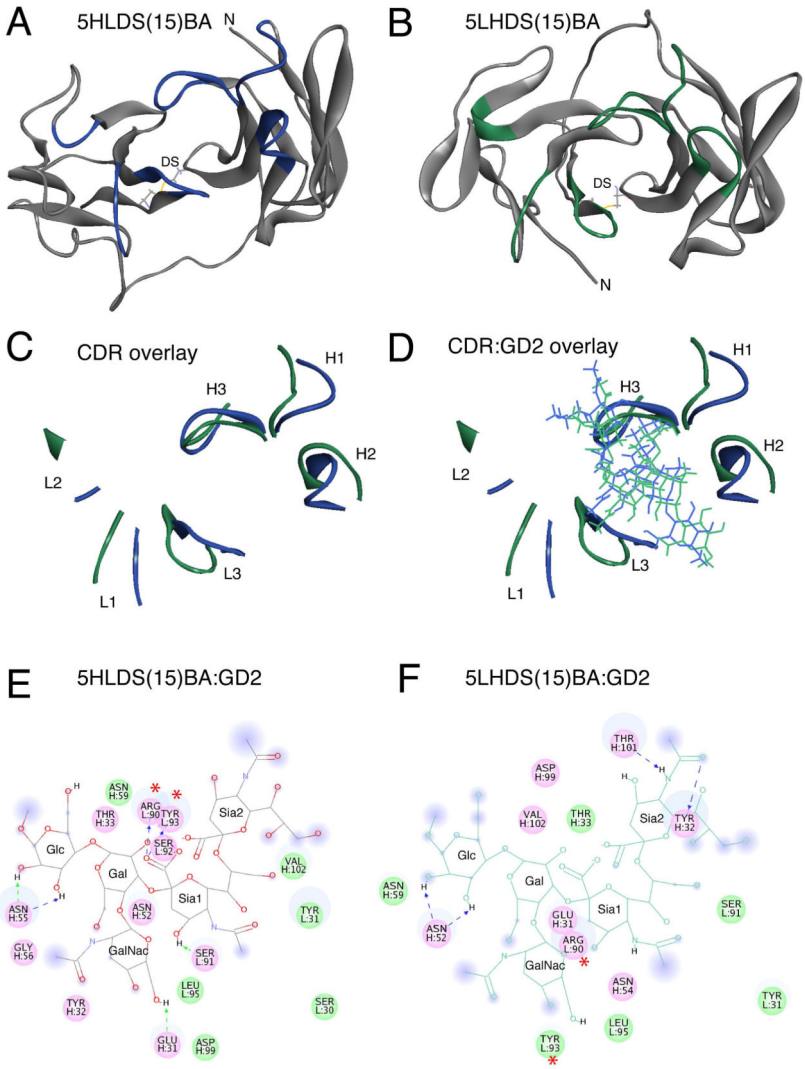

Figure 1. Molecular Modeling of anti-GD2 5F11-scFv in the 5HLDS(15)BA and 5LHDS(15)BA constructs

Molecular Modeling of anti-GD2 5F11-scFv in the 5HLDS(15)BA and 5LHDS(15)BA constructs. **A**) Ribbon diagram of 5F11-scFv in 5HLDS(15)BA (5F11 VH - linker - VL - disulfide stabilized), where VH-VL disulfide stabilizing residues are shown in stick rendering, and CDR main chain residues are shown in Blue. **B**) Ribbon diagram of 5F11-scFv in 5LHDS(15)BA (5F11 VL - linker - VH - disulfide stabilized), where VH-VL disulfide stabilizing residues are shown in stick rendering, and CDR main chain residues are shown in Green. **C**) Overlay of CDR loops of 5HLDS (Blue) and 5LHDS (Green). **D**) Overlay of CDR residues with docked model of GD2 for 5HLDS(15)BA:GD2 (Blue) and $5LHDS_{15}$BA:GD2 (Green). **E**) Interaction diagram of 5HLDS(15)BA:GD2 and **F**) Interaction diagram of 5LHDS(15)BA:GD2. Interacting residues are displayed as colored discs. Residues with H-bonding, charged or polar interactions are colored in magenta. Residues having van der Waals interactions are colored in green. H-bonds, and charge-charge interactions are displayed as dashed lines. The solvent accessible surface is shown as a diffuse background circle with the radius proportional to the exposure. The per residue

interaction energies are shown in **Supplemental Table III**. The residues with the largest contributions to the interaction with GD2 are L: Arg90 and L: Tyr93, which are significantly reduced in 5LHDS(15)BA:GD2 (noted with *).

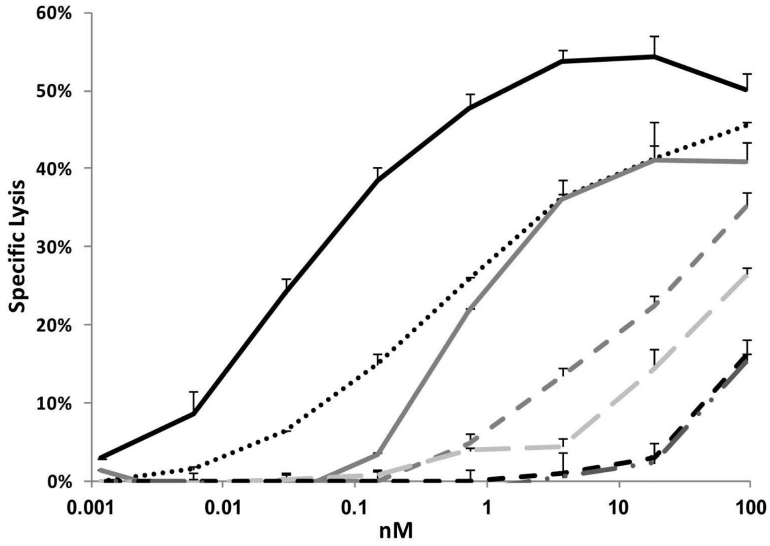

Figure 2. T cell cytotoxicity of LAN-1 cells in the presence of 5F11-BsAbs

T cell cytotoxicity of LAN-1 cells labelled with ^{51}Cr was assayed in the presence of increasing concentrations of 5F11-BsAbs. Specific lysis was measured by ^{51}Cr release in supernatant counted by a γ-counter.

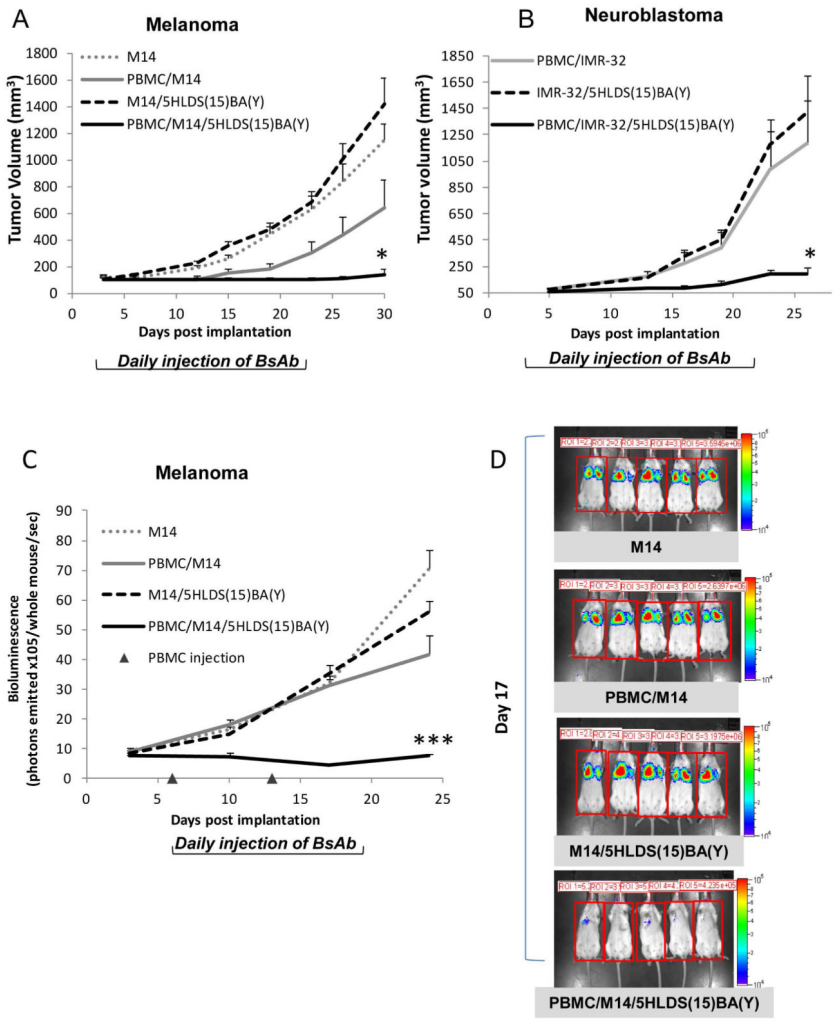

Figure 3. In vivo tumor therapy using 5HLDS(15)BA(Y)

BALB-Rag2-/-IL-2R-rC-KO (DKO) mice were implanted with (**A**) 3×10^6 M14 (melanoma) only or mixed with 3×10^6 human PBMC (**B**) 5×10^6 IMR-32 (neuroblastoma) only or mixed with 5×10^6 human PBMC on day 0 and then treated with 5HLDS(15)BA(Y) at 20 μg daily intravenously starting on day 3 for a total of 20 days. Tumor size was measured twice a week and calculated with the formula: volume = $(\text{width})^2 \times \text{length}/2$. *$P < 0.05$, unpaired t test. (**C and D**) M14 cells (1.5 million) were injected into DKO mice intravenously, treatment with intravenous BsAb was initiated on day 6 daily for a total of two weeks. PBMC were injected intravenously on day 6 and 13. Tumor growth was assessed by luminescence once a week starting on day 2. ***$P < 0.001$, unpaired t test.

Table I

Different formats of 5F11-BsAbs (BA).

Name	Anti-GD2 scFv	Linker	Anti-CD3 scFv	Formats
5HL(15)BA	5F11-VH-VL	(GGGGS)3	huOKT3-VH-VL	
5HLDS(15)BA	5F11-VH-VLDS	(GGGGS)3	huOKT3-VH- VL	
5LH(15)BA	5F11-VL-VH	(GGGGS)3	huOKT3-VH-VL	
5LHDS(15)BA	5F11-VL-VHDS	(GGGGS)3	huOKT3-VH-VL	
5HLDS(5)BA	5F11-VH-VLDS	(GGGGS)1	huOKT3-VH-VL	
5LHDS(5)BA	5F11-VL-VHDS	(GGGGS)1	huOKT3-VH-VL	
5HLDS(15)BA (Y)	Y-5F11-VH-VLDS	(GGGGS)3	huOKT3-VH-VL	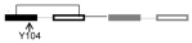

VH-VL or VL-VH: orientation of VH and VL in 5F11-scFv and hOKT3-scFv. DS: Disulfide bond stabilization, indicated by square brackets. 5HLDS(15)BA(Y) is the same format as 5HLDS(15)BA with one additional affinity maturation mutation P104Y in the CDR region[21].

Table II

Relative binding in percent of 5F11-BsAb to GD2 and CD3.

5F11-BsAb constructs	GD2 binding (ELISA)	CD3 binding (ELISA)	CD3 binding (flow cytometry)	antigen binding ranking
5HLDS(15)BA	100	100	100	2
5HL(15) BA	15	30	24	5
5LH(15)BA	73	100	92	3
5LHDS(15)BA	1	15	2	7
5HLDS(5)BA	5	22	4	6
5LHDS(5)BA	32	66	58	4
5HLDS(15)BA (Y)	143	115	101	1

GD2 and CD3 binding were measured by ELISA. ELISA OD was normalized as % of binding of 5HLDS(15)BA to these antigens. CD3 binding was also assayed by flow cytometry against T cells. MFI (Mean fluorescence Intensity) was normalized as % of binding of 5HLDS(15)BA to Jurkat cells.

Table III

5HLDS(15)BA(Y) redirected T cell cytotoxicity of human tumor cell lines

Tumor type	Cell lines	GD2 expression (MFI)	Maximum level of lysis	Tumor cytotoxicity (EC50)(nM)
Melanoma	SKMEL-1	38	36%	0.01
Neuroblastoma	LAN-1	201	52%	0.04
Neuroblastoma	NMB-7	127	60%	0.05
Melanoma	M14	50	50%	0.09
Neuroblastoma	BE(1)N	94	46%	0.17
Neuroblastoma	IMR-32	128	58%	0.20
Melanoma	HT-144	13	35%	0.48
Small cell lung cancer	NCI-H524	66	58%	0.61
Neuroblastoma	SKNJC2	6	25%	0.86*
Melanoma	SKMEL28	8	28%	2.20*
small cell lung cancer	NCI-H69	27	39%	3.16*
Breast Cancer	MDA-MB-468	6	13%	3.89*
small cell lung cancer	NCI-H196	8	7%	> 185
small cell lung cancer	NCI-H345	7	2%	>185

GD2 expression of cell lines were expressed as mean fluoresce intensity. Cytotoxicity assays (^{51}Cr release) were carried out with cultured T cells at E: T ratio of 10:1. Maximum level of lysis was measured at a 18.5 nM concentration of 5HLDS(15)BA (Y). EC50 was calculated using Sigma plot 8.0.

*Numbers were extrapolated by Sigma plot 8.0.